Optimisation and durability in fabric cast 'Double T' beams

J J Orr[1], A P Darby[1], T J Ibell[1] and M C Evernden[1]

[1] *Department of Architecture and Civil Engineering, University of Bath, Bath, BA2 7AY, UK.*

By replacing orthogonal concrete moulds with a system formed of flexible sheets of fabric it is possible to construct optimised, variable cross section concrete elements that can provide material savings of up to 40% when compared to an equivalent strength prismatic member, and thereby offer the potential for significant embodied energy savings in new concrete structures. This paper presents the salient results of two sets of tests recently undertaken at the Building Research Establishment Centre for Innovative Construction Materials (BRE CICM) at the University of Bath that considered 1) the design, optimisation and construction of 4m span double 'T' beams and 2) the surface properties of concrete cast into a permeable fabric mould. The results of these tests demonstrate how a fabric formwork construction system may be used to facilitate a sustainable future for concrete construction, providing a design method by which structurally optimised elements may be cast in an economical manner while also providing significant durability and visual benefits that combined provide an advantageous whole-life performance for fabric formed concrete that is unmatched by many other construction systems.

1 Introduction

The construction of optimised concrete structures, offering reductions in material use and embodied carbon, has been a research goal the University of Bath for some time. Recent research demonstrates that fabric formwork can provide a construction method to facilitate such an ideal.

Presented in this paper are the results of tests on a series of 4m span, structurally optimised, 'Double T' beams cast using fabric formwork. The design process, construction, testing and results are presented. It was found that through a simple optimisation process elements with material consumptions some 35% less than an equivalent strength prismatic element could be created.

In addition to the benefits a flexible mould brings in terms of material use reduction, this paper also demonstrates how fabric formwork can be used to create durable, visually appealing, concrete structures. These two advantages, arising from the manner in which concrete cures in the fabric mould, ensure a significant advantage in the whole life performance of fabric cast concrete. Combined with the previously noted reductions in material use, fabric formwork may thus provide a means by which architects and engineers can create low-carbon concrete structures to facilitate a sustainable future in concrete construction.

1.1 Background

The language and technology of concrete construction has changed dramatically over the past two thousand years - from dome of the Pantheon, through its renaissance in the 1800s, and up to the work of Nervi and other modern masters of this fluid material. Throughout this, concrete has been cast almost exclusively into wooden or steel moulds to create prismatic elements. Nervi himself noted that:

'*although reinforced concrete has been used for over a hundred years and with increasing interest during the last few decades few of its properties and potentialities have been fully exploited so far...the main cause of this is a trivial technicality: the need to prepare wooden forms*' (Nervi, 1956)

This triviality pervades the minds of Engineers even today, with increased cost being associated with concrete structures that deviate from the use of flat panels of timber or steel as formwork. Despite this,

concrete remains one of the most widely used man made materials in the world, with global production of cement approaching 2.8x10⁹t in 2008 (USGS, 2008). Cement accounts for a large proportion of the world's raw material expenditure, reaching nearly 33% of the total in 2008 (USGS, 2011). Although concrete has a relatively low embodied energy (Hammond and Jones, 2008) its rate of consumption means that cement manufacture alone is estimated to account for some 3% of global CO2 emissions (WRI, 2005).

Against a backdrop of carbon dioxide emissions reduction targets, a recognition of the impact construction has on the environment and an increasing focus on sustainability, design philosophies centred around the need to put material where it is required are becoming increasingly desirable.

2 Optimised construction

In light of the concerns, ambitions and targets outlined above, research at the University of Bath has focused on how reductions in the embodied carbon of new concrete structures may be achieved. In addition to work considering realistic loading and serviceability conditions, research at the BRE CICM has considered the structural mechanics of optimised concrete structures such that they may be cast in fabric formwork.

Following from previous work by the authors (Orr et al., 2011b) a series of tests were recently been completed in which 4m span double T beams subjected to uniformly distributed loads were optimised and constructed using fabric formwork. The elements were calculated to consume at least 35% less concrete than an equivalent strength prismatic element.

2.1 Double T Design

The design and optimisation of two four-metre span Double T beams was undertaken to the loading envelope shown in Figure 1(left) using a sectional design approach which aimed to satisfy the bending and shear requirements of the beam at every point along its length.

The flexural requirements of the beam were assessed using the provisions of BS EN 1992-1-1 (2004), as summarised in Figure 1(right) (partial safety factors are set to 1.0). A concrete strength of 30MPa and steel yield strength of 500MPa was assumed.

Shear design was also undertaken using the provisions of BS EN 1992-1-1 (2004). In Beam 1, any vertical components of force in the longitudinal steel were ignored, while in Beam 2, this steel was able to act as a 'bent up bar'.

Each section was additionally checked using the design provisions of the modified compression field theory, described in detail by Collins *et al.* (1978). This has been shown to be more effective than BS EN 1992-1-1 (2004) in many situations (Collins et al., 2008, Orr et al., 2012c). It should be noted that the design requirements for this beam were governed primarily by flexural requirements; additional work considering tapered beams loaded predominantly in shear is considered separately (Orr et al., 2012c), where the design approach of BS EN 1992-1-1 (2004) is seen to be unconservative in some situations for tapered steel reinforced concrete beams.

The resulting designs are shown in Figure 2, where the placement of both flexural and transverse reinforcement has been optimised to provide the required load capacity and to facilitate a practical construction method.

2.2 Construction

The Double T beams were cast in the 'double keel' fabric mould shown in Figure 3. Four flat sheets of fabric were firmly secured between two 'keels', with flat timber plates used to form the support points. The steel reinforcement was hung in the mould prior to casting, after which the beam was lifted and the fabric stripped from it. The fabric used in this test is described in Table 1. Average concrete compressive strengths measured from three cubes tested prior to each beam test are given in Table 2. Although the same mix design was used, differences between the two deliveries were seen, although these will have only a small effect on the flexural strength of the beam.

Table 1: Fabric properties.

Material (warp/weft)	Tensile strength (warp/weft)	Elongation (warp/weft)	Pore size
Polyester	54kN/m	25%	423µm

Table 2: Concrete compressive strengths.

	Beam 1	Beam 2
Compressive Strength (MPa)	23.7MPa	31.8MPa

2.3 Testing

Testing of the Double T beams was undertaken as shown in Figure 4, where seven point loads were applied to the beam to represent the design loading envelope. Beam 1 was tested to failure in Load Case 1 (LC1) while Beam 2 was tested in LC1 to 60% of its design load before being unloaded and tested to failure in Load Case 2 (LC2), as shown in Figure 1(l) and Figure 5(r).

Beam 1 reached a peak load of 33kN in LC1, after which considerable ductility in the beam was seen (maximum midspan displacement of 87.6mm), Figure 5(l). The beam exceeded the predicted design load by 16%, an increase explained by considering the actual yield strength of the steel and concrete compressive strength when compared to the values assumed in design. Well distributed cracking along the beam was recorded during testing, and final failure was recorded in crushing of the top slab, as shown in Figure 5(r).

The results of Beam 2 tested in LC2 are shown in Figure 5(l), where the displacement 1m from the roller support is plotted against the total applied load. The results from Beam 2 in LC1 are plotted as a comparison to show the residual deformation of the beam prior to testing in LC2. In LC2 Beam 2 again exhibited excellent ductility and after reaching a maximum load of 30kN displayed a plateau of deflection up to approximately 107mm. Given the asymmetric loading, the beam deformation was correspondingly asymmetric. Final failure for the beam was seen in crushing of the top concrete slab.

The beam design has thus been shown to perform well under the applied loading and has stayed within the design envelope. Predictions of the load-deflection behaviour of the two beams were made by considering the curvature of each section under loading and following a routing of double-integration to determine the deflections.

2.4 Conclusions

The tests presented in above show that efficient beams with reduced material use can be realised using fabric formwork. Such results suggest significant reductions in embodied energy are achievable when using fabric formwork, as demonstrated further by Lee (2010).

The construction of the 4m span double tee beams was complicated by the large number of links, each of which had different overall dimensions. Whilst this slowed down the construction of the prototype elements, such a construction process could add significant labour time and in turn, cost. This additional cost could potentially outweigh the economic advantage of the reductions in material use that have been achieved, hampering the implementation of fabric formwork in the cost conscious construction industry.

Two further approaches were therefore taken to address this issue. The first approach was to use fibre reinforced polymer reinforcement as an alternative to steel bars. This was successfully achieved using Carbon Fibre grids as shear reinforcement (Orr et al., 2011a). The second approach was to investigate the use of advanced concrete technology to facilitate the removal of all the internal transverse reinforcement. This was achieved using an ultra high performance fibre reinforced concrete supplied by Lafarge and is described by Orr *et al.* (2012b).

The Double T beams presented in this paper demonstrated the desired flexural response under loading. As has been described above, previous work (Garbett, 2008) has exposed potential problems with the way that existing design methods deal with the shear behaviour of non-prismatic concrete elements. To begin to address these concerns, which are of particular importance for fabric formed elements, tests undertaken on tapered reinforced concrete beams comparing the shear behaviour of elements designed using the variable angle truss model of BS EN 1992-1-1 (2004) with those designed using the compressive force path concept have recently been published to supplement the work presented in this paper (Orr et al., 2012c).

The successful design and construction of the fabric formed Double T beam demonstrates that this design and construction method may be used to create materially efficient concrete structures. The tests have thus demonstrated how fabric formwork may be used to achieve a sustainable future in the concrete construction industry.

In addition to the benefits of material use reduction, fabric formwork offers potential durability, and therefore whole-life, advantages. This aspect of the technology is considered in detail in §3.

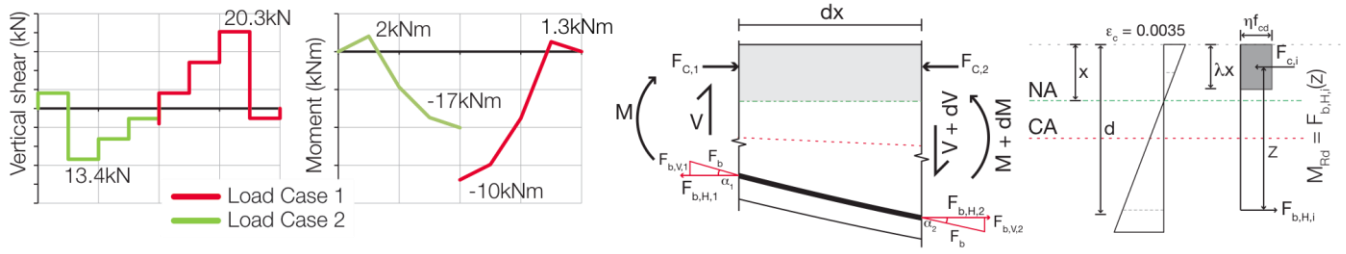

Figure 1: Load envelope (left) and basis of design method for flexure (right).

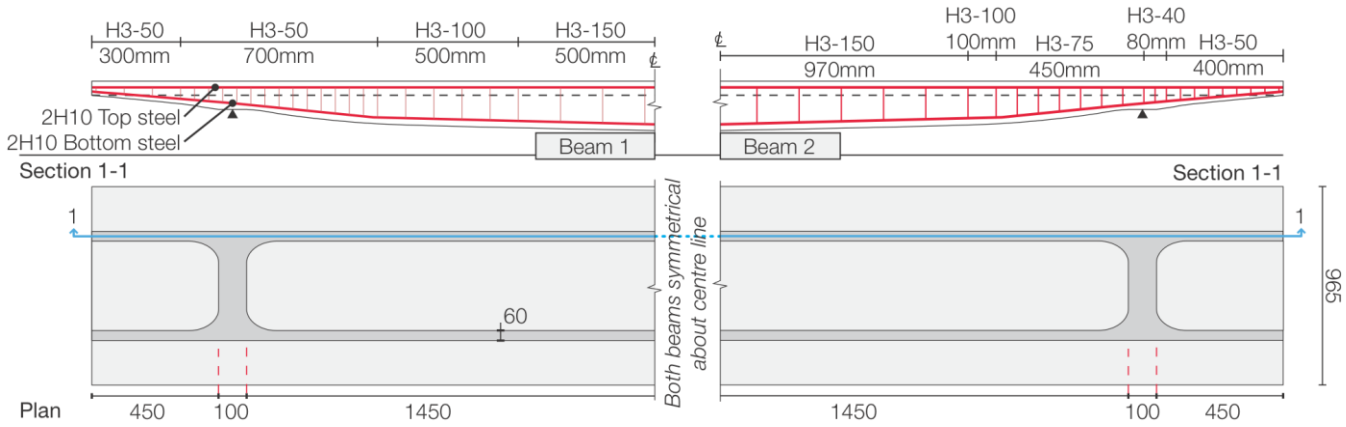

Figure 2: Beam 1 and Beam 2 Designs and reinforcement layouts

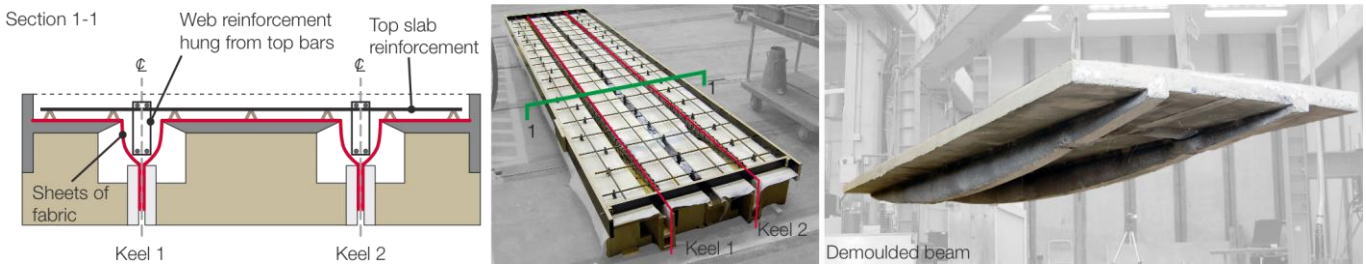

Figure 3: Double keel mould (l), construction (centre) and resulting beam (r).

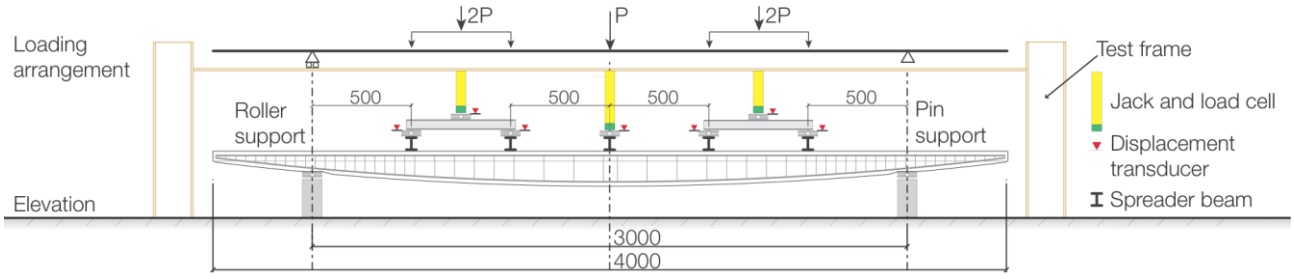

Figure 4: Test setup for Beams 1 and 2

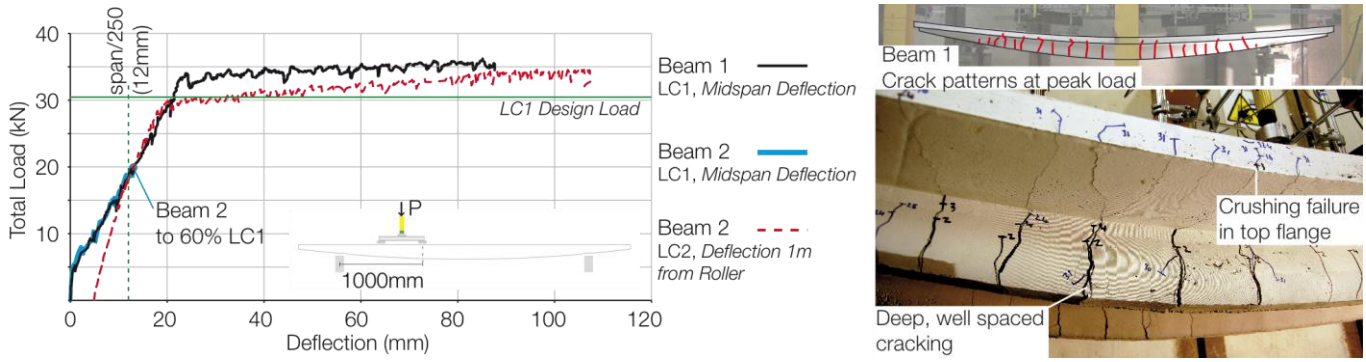

Figure 5: Load-deflection results for Beam 1 and Beam 2 in LC1 and LC2 (l); Cracking at failure, Beam 1 (r).

3 Durability

3.1 Introduction

By allowing water and air to be expelled from a concrete element as it cures, permeable formwork systems provide concrete with improved durability due to its denser microstructure and reduced *water:cement* ratio in the cover zone (McCarthy et al., 2001). However, commercially available permeable formwork systems require the fixing of permeable and draining layers to the inside of conventional structural formwork. The alternative use of a single flexible fabric formwork system for the creation of optimised, durable structures therefore offers real advantages for designers.

The results of carbonation and chloride ingress are summarised before the results of sorptivity tests and Scanning Electron Microscopy imaging are presented. Combined, the results demonstrate that fabric cast concrete can be used to create durable structures that offer significant whole-life benefits for concrete construction. Visual benefits are also seen in the fabric cast surface texture, where the cement rich surface zone provides a darker concrete colour and the absence of surface defects provides a visually appealing finish (Figure 6).

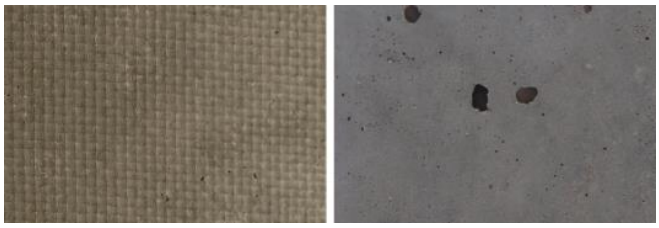

Figure 6: Fabric cast (left) and Timber cast surface (right), from the same concrete mix.

3.2 Carbonation

Steel reinforcement is protected from corrosion by the high pH of its surrounding concrete. Carbonation of the concrete mix, precipitated by the presence of carbon dioxide in the atmosphere, reduces the alkalinity of the concrete through the conversion of calcium hydroxide ($Ca(OH)_2$) in the cement paste to calcium carbonate ($CaCO_3$) and water. This detrimental process occurs primarily by gaseous diffusion through air filled pores, and is often described using Fick's law.

To determine the relative resistance of fabric and steel cast concrete to carbonation, accelerated testing was undertaken by exposing samples to an atmosphere of elevated CO_2. The NordTest NT 357 (1989) method was followed, in which a concentration of 4% is used. By comparison atmospheric CO_2 is currently estimated at 392 parts per million (Tans, 2010), or 0.039% of the atmosphere by volume. Under such a regime Dunster (2000) suggests that seven days exposure is equivalent to 12 months under natural conditions.

Modified cube moulds, in which one face was cast against a drained fabric surface and the other against steel, were used to provide a comparative test method, full details of which are provided by Orr *et al*. (Orr et al., 2012a) . Salient results from this test series are summarised in Figure 7, where the depth of carbonation recorded on the fabric and timber faces at 7, 14, 28, 90 and 180 days (representing 1, 2, 4, 12.8 and 25.7 years) is shown.

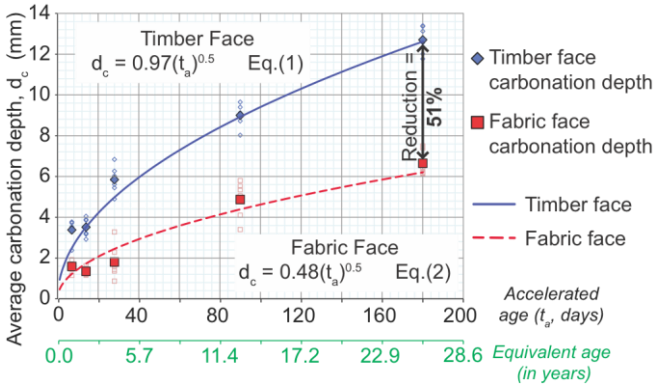

Figure 7: Summary of carbonation measurements.

3.2.1 Analysis

Models for the prediction of concrete carbonation, which occurs primarily by gaseous diffusion through air filled pores and is often described using Fick's law (Steffens et al., 2002), can be summarised by Eq.(3) (Liang et al., 2002).

$$C_i = B_i t_a^{0.5} \qquad (3)$$

Where C is the carbonation depth in mm and B is the coefficient of carbonation for the face i (fabric or timber cast); t_a is the accelerated exposure time in days.

Equations were determined to compare the rate of carbonation in timber and fabric cast concrete members. These are given by Eq.(1) and Eq.(2), plotted on Figure 7. Values for the coefficients of carbonation B_{timber} and B_{fabric} calculated from the accelerated test data are thus shown to be reduced by 51% for concrete cast against fabric formwork. Where estimated in-situ carbonation depths are required, Eq.(1) and Eq.(2) should be modified to account for the accelerated nature of the tests.

3.2.2 *Conclusions*

Accelerated carbonation tests carried out on specially prepared cubes showed considerable improvements in surface durability and resistance to carbonation for the fabric cast surface. After 180 days, the fabric cast surface had a much-reduced average carbonation depth than the equivalent timber cast concrete. Fabric cast concrete may thus be used to provide concrete structures with reduced cover distances that retain the same service life as a conventionally cast element with greater cover. Further work is now underway to quantify the improvements shown here for a range of concrete strengths and fabric types in order to provide complete guidance for designers.

3.3 Chloride ingress

Unsaturated concrete will absorb a chloride solution into unfilled spaces in the surface by capillary action (Bamforth and Price, 1997). Upon drying, water in the chloride solution evaporates, leaving the salts behind which then build up over time. A range of factors affect the rate of chloride ingress into concrete structures, including the concentration of the chloride solution to which the structure is exposed and the resistance of the concrete cover zone to chloride penetration. Changes to the surface permeability of fabric cast concrete may therefore be beneficial in increasing resistance to chloride ingress.

The potential for increased chloride resistance in fabric cast concrete was investigated by chloride ingress tests on ø100mm cylindrical concrete specimens, which were tested in accordance with the method described in NT Build 443 (1995b).

Seven cylinders (four of which were cast in a fabric mould) were exposed to a solution of sodium chloride (165±1g NaCl per dm^3 water) for either 53 or 90 days. Nine samples were then taken at incremental depths (up to 20mm) from each cylinder and subjected to Volhards titration, undertaken in accordance with NordTest 208 (1995a). Non-linear regression analysis of these results was used to determine the non-steady state chloride diffusion coefficient (D_{nss}) for the timber and fabric cast concrete.

These results are summarised in Figure 8, where reductions in D_{nss} of 58% after 53 days and 41% after 90 days were seen when comparing the fabric and steel cast samples.

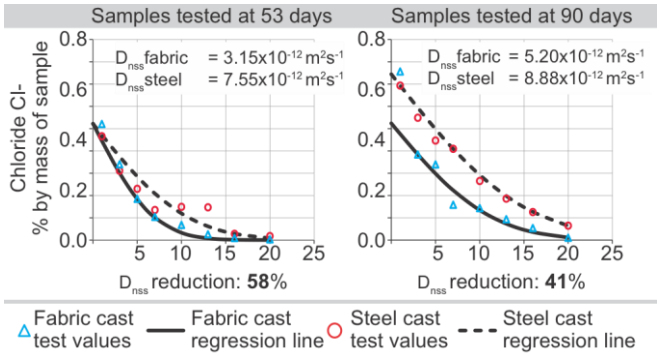

Figure 8: Chloride ingress profile summary.

3.3.1 *Conclusions*

Concrete cylinders cast in steel and fabric moulds were used to determine the relative resistance to chloride ingress of the fabric cast concrete, and the results showed significant improvements in the fabric cast specimens. There is thus reasonable confidence that fabric cast concrete provides better resistance to chloride ingress by diffusion. However, it should be recognised that only sixty-three titration tests were undertaken, and only one fabric type and concrete mix was tested.

Since the primary resistance of concrete to chloride ingress is through the binding of the chlorides (Schiessl and Lay, 2005), the improved performance of fabric cast concrete suggests it exhibits a greater binding capacity, which in turn suggests that there is a greater concentration of cement in the surface zone. Cement binding increases the formation of Friedel's salt in the surface zone, the structure of which further retains chlorides to protect against chloride ingress (Yuan et al., 2009). Although this formation was not directly measured, its impact would be to inhibit the transport of chloride ions into the concrete structure, a result that may be inferred from the tests presented above.

3.4 Sorptivity

In much of the literature, the sorptivity (the rate of liquid absorption by capillary action) of a hydraulic cement concrete is related to its durability characteristics, as described by Hall (1989). In light of the advantageous tests described above, sorptivity tests were undertaken to determine how this aspect of the concrete behaviour is affected by the use of a permeable mould.

Sorptivity profiles for porous materials in unidirectional tests show a water absorption profile that advances with the square root of time (Gummerson et al., 1979).

The result is modelled in much of the literature by the non-linear diffusion equation given in Eq. (4) (Lockington and Parlange, 2003). Eq.(4) has the solution given by Eq.(5), provided there is a uniform initial water content and the specimen has is placed in a reservoir (i.e. has a wet face) at the position $x = 0$.

$$\frac{\partial\theta}{\partial t} = \frac{\partial}{\partial x}\left\{D(\theta)\frac{\partial\theta}{\partial x}\right\} \quad (4)$$

$$x(\theta,t) = \phi(\theta)\sqrt{t} \quad (5)$$

Where θ is the water content, D(θ) is the hydraulic diffusivity (mm^2/s), t the time (s) and x the spatial coordinate (mm).

The sorptivity is thus often given simply as the volume of water absorbed by a specimen, Eq.(6) (Hall, 2007) and gives a linear increase with the square root of time.

$$i = A + S\sqrt{t} \quad (6)$$

Where i is the cumulative volume of absorbed liquid at time t and A is a constant.

Although sorptivity testing may be carried out on cementitious materials, there is evidence to suggest that the $t^{0.5}$ relationship does not hold when there is potential for chemo-mechanical interaction with the material (Lockington and Parlange, 2003). This may be avoided through the use of an organic liquid such as n-decane, which does not interact with concrete in the same way as water (Taylor et al., 1999). However, in the following test series the ASTM C1585 (2004) method is used, which allows the use of water but provides a bi-linear analysis method.

3.4.1 Test method

Twelve concrete cylinders (ø100 x 200mm) were used to determine the sorptivity characteristics of fabric and timber cast concrete, both at the cast face and at 25mm from the cast face, as described in Table 3. Six specimens with a fabric base and six with a steel base were cast. Concrete strengths are provided in Table 4.

The specimens were demoulded after 24 hours and a 50mm deep section was cut from six (three steel 'S' and three fabric 'F') samples, denoted S1-S3 and F1-F3. The remainder had a 25mm section cut from the cast surface, with a 50mm deep section then cut from the remaining prism to make samples S4-S6 and F4-F6. The 50mm deep discs were stored at 50±2ºC for 3 days. After curing for a further 28 days in a sealed container, each sample was weighed, measured and its sides were coated in paraffin wax. A plastic bag was secured over the unwaxed face opposite to the similarly unwaxed test face. Each specimen was placed in a water bath, filled to the level shown in Figure 9 with water at 23±2ºC, and supported off the base of the container. The mass of each specimen was then determined at the following time intervals: 60±2s, 5min±10s, 10±2mins, 20±2mins, 30±2mins and 60±2mins. After 1 hour, the measurements were taken at each hour up to 6 hours, then once a day until 7 days after the first test.

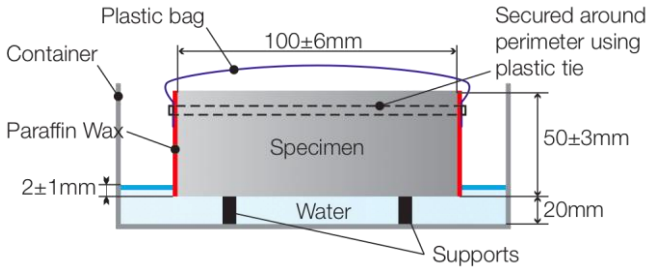

Figure 9: Setup for sorptivity testing.

Table 3: Summary of sorptivity test specimens

Sample	Cast face	Test location
S1, S2, S3	Steel	Cast surface
F1, F2, F3	Fabric	Cast surface
S4, S5, S6	Steel	25mm from cast surface
F4, F5, F6	Fabric	25mm from cast surface

Table 4: Recorded concrete strengths.

Sample	1-3	4-6
28 day compressive strength (MPa)	38.1	35.2

3.4.2 Analysis

Following ASTM C1585 (2004), the results were analysed by considering linear relationships between the values of $t^{0.5}$ and the change in mass of the specimen. The absorption, *I*, is given by Eq.(7). Two periods of water absorption are defined - an initial absorption up to 6 hours from the test start, followed by secondary absorption to the test end. The area of each sample is the projected area of the cylinder.

$$I = \frac{m_1}{a/d} \quad (7)$$

Where I is the absorption (in mm); m_1 is the change in specimen mass in grams at the time t; a is the exposed area of the specimen in mm^2 and d is the density of water in g/mm^3 (taken here as $0.001g/mm^3$).

$$I = S_i\sqrt{t} + b \quad (8)$$

Where S_i is the initial or secondary absorption and *b* is a constant.

The initial water absorption is calculated from a line of best fit plotted over the first six hours of data using a linear regression analysis, with all graphs plotted as mm versus $t^{0.5}$ (correlation coefficient of >0.98). The secondary rate of water absorption is taken as a linear relationship in the remaining data and the primary and secondary rates of absorption are calculated as shown in Eq.(8). One result (Sample S1) is shown in Figure 10 (excellent R^2 correlation was seen in all tests), with a full summary of all data being given in Table 5.

Table 5: Summary of sorptivity test results

Samples	S_i	S_s
S1-S3	0.021	0.0003
F1-F3	0.023	0.0003
S4-S6	0.0206	0.0003
F4-F6	0.0211	0.0003

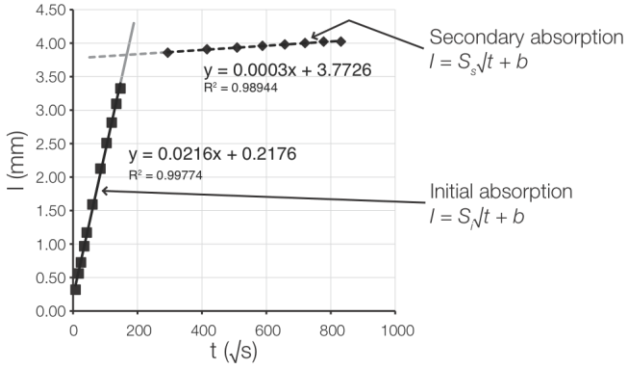

Figure 10: Typical sorptivity plot for Sample S1 showing bi-linear relationship over a period of 7 days.

The results show little difference in the recorded values of the coefficients S_i and S_s. However, by considering the difference in the values of *I* recorded at each time step, significant differences between the fabric and steel cast faces can be seen.

The percentage difference in *I* recorded at the fabric and steel faces at each time step for Samples 1-3 and 4-6 is shown in Figure 11. It is seen that at the cast face (Samples 1-3) the fabric cast surface has absorption rates up to 40% lower than the steel cast surface. This advantage rapidly drops off, such that when measured over a six-hour period the values of S_i are almost identical. In Samples 4-6, only very small differences are recorded over the test duration, suggesting that any changes in concrete microstructure caused by the fabric mould are confined to a small zone (<25mm) from the cast face.

The importance of this difference in test duration is highlighted by Balayssac (1992) who showed that the initial rate of water absorption is dependent primarily on larger pores (up to 1.25µm) while the longer term rate can provide a measure of the presence of smaller pores (average size 0.04µm). The results presented here thus suggest that whilst there are less large pores in the fabric cast concrete, the size of the smallest pores is not reduced and hence over a longer time, when the smaller pores dominate, the fabric and steel cast concretes have similar sorptivity behaviours.

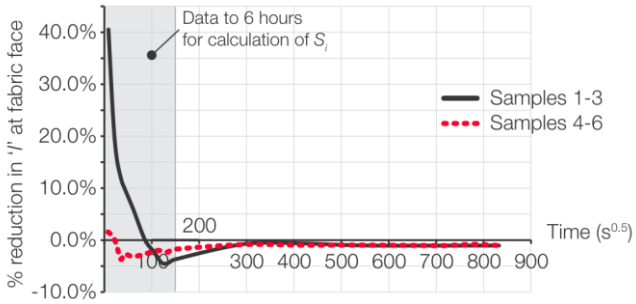

Figure 11: Average value of 'I' over the test period

3.4.3 Conclusions

The collected sorptivity test data has been used to determine long term (up to 8 days), medium term (up to 6 hours) and short term (up to 1 hour) behaviour of the fabric cast concrete. In the short term, the data has been used to suggest that fabric cast concrete has fewer large pores and thus a smaller average pore size. Medium and long-term data suggests little difference exists in the sorptivity behaviour using water of the fabric and steel cast specimens.

To determine if the smaller average pore sized inferred from these tests is accompanied by an increase in cement at the surface zone (as suggested by the chloride ingress results), tests were undertaken using a scanning electron microscope (SEM) and energy-dispersive X-ray spectroscopy (EDS), where images at high magnification and analysis of compounds present at the surface of both fabric and timber cast concrete were collected.

3.5 SEM Data

A small sample of a series of tests undertaken at the University of Bath are presented in the following section, in which SEM and EDS were used to determine how the cement content of the fabric cast concrete is altered at the cast face.

Four small samples were cut from the fabric and timber cast faces of a larger prism, which was cast in a specially constructed mould. The samples are identified as shown in Figure 12.

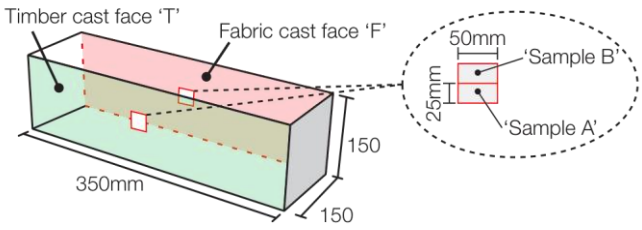

Figure 12: SEM Sample Locations and referencing

The samples were stored at 20ºC, 60%RH for 56 days prior to testing. They were then degassed for 96 hours to achieve the required vacuum level for SEM imaging. Samples F-A and T-A were coated in conductive gold using a sputter coater and were imaged at progressively increasing magnifications. Samples F-B and T-B were coated in carbon and were then both imaged at increasing magnification and subjected to energy-dispersive X-ray spectroscopy to determine their chemical characteristics. The resulting images and EDS results are presented in the following sections.

3.5.1 Results

Initial imaging at increasing magnification of the two cast faces is shown in Figure 13. In the fabric cast an imprint of the fabric weave structure on the surface is evident and the characteristic surface texture of the fabric cast concrete can be seen at all magnifications, creating weave areas and intersection areas between the individual fibre locations.

EDS was undertaken on the samples with the aim of determining the composition at the cast face. This was repeated twice for each sample, and some typical results showing compositional information plotted as a 3D chart is shown in Figure 14.

Each of the element maps was created using INCA software to show the distribution of eight elements (Sodium, Magnesium, Aluminium, Silicon, Sulphur, Potassium, Calcium and Iron). Each of the maps contains 12,288 pixels, with each given an intensity based on the percentage by weight of each element present at the surface.

The average and median values for each element by weight percentage were obtained from the collected matrix data, with median data information presented in full in Table 6. From these it can be seen that the mapped area of the fabric face (Sample F) had approximately 14% more Calcium, and 43% less Silicon, present at the surface, with the average values showing similar results (median values being preferred for comparison here as they reduce the influence of any outlying results).

Table 6: Median value of each element in weight %.

Sample	Na	Mg	Si	Al	S	Fe	Ca	K
F-A, F-B	0.046	0.187	8.777	1.713	0.050	1.000	73.140	3.403
T-A, T-B	0.146	0.600	15.424	3.942	0.082	1.072	63.945	4.378
% Change T to F	-68%	-69%	-43%	-57%	-38%	-7%	14%	-22%

The above results provide a clear indication of the changes in surface properties that arise in fabric cast concrete. The SEM imaging and EDS results show significant changes in the surface topology of fabric cast concrete, in addition to the distribution of elements at the surface zone. Higher concentrations of Calcium and reductions in Silica concentrations suggest smaller cement particles are collected at the surface zone, providing a dense region with reduced pore sizes that contribute to the increased resistance to carbonation and chloride ingress seen in durability tests presented above.

Previous work (Price, 2000) shows a link between *water:cement* ratio and the improvements in surface properties found in permeable formwork. The challenge of measuring *water:cement* ratios in hardened concrete is, however, considerable. Much of the work undertaken to date uses optical techniques such as those described by Skjovsvold (1991, cited by Price, 2000) and codified in NT Build 361 (1999). Using fluorescent dyes, a range of concretes with known *water:cement* ratios must be compared to the test specimen before its *water:cement* ratio can be estimated. Considerable preparation time is required, and the test accuracy is entirely dependent on the number of comparators that are cast. For this reason, this technique was not employed in these tests.

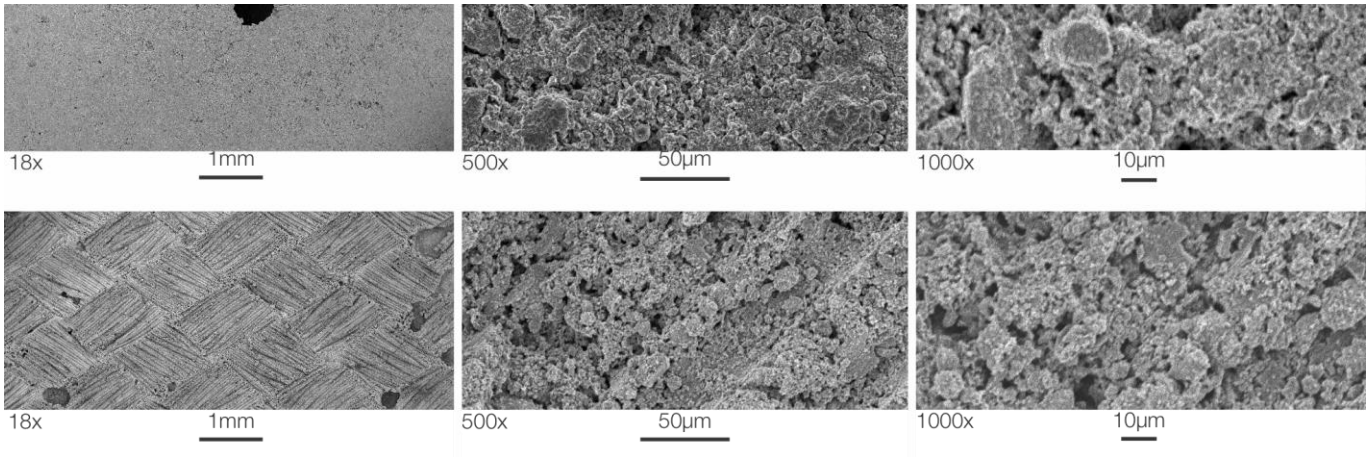

Figure 13: Sample of SEM data at increasing magnification for timber (top) and fabric (bottom) faces.

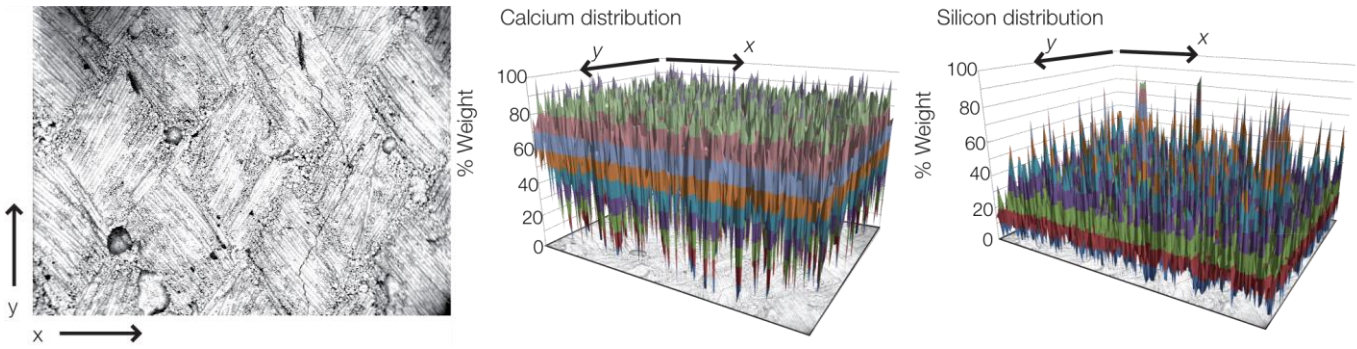

Figure 14: Sample of EDS data for a fabric cast face showing distribution by Weight% of two elements, Ca (left) and Si (right).

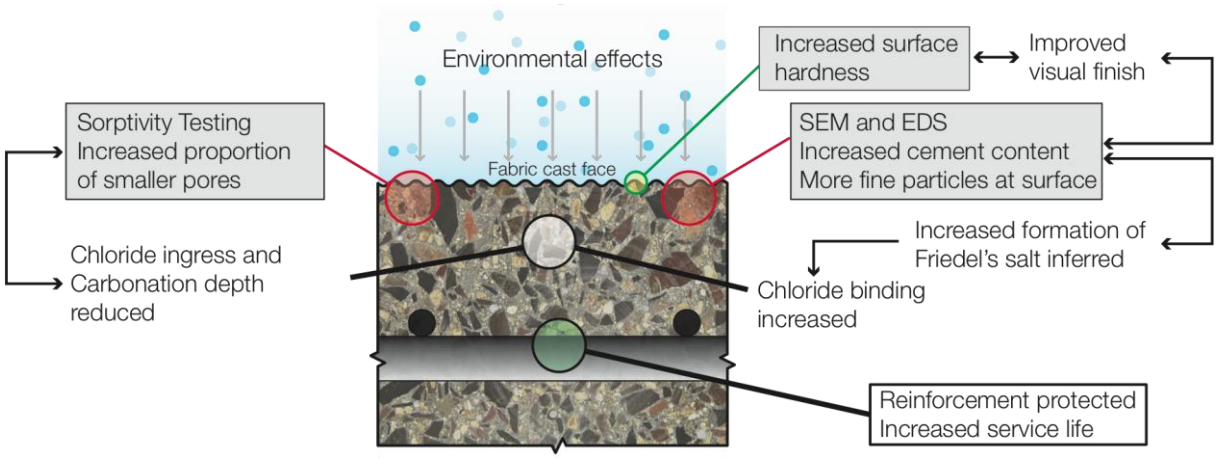

Figure 15: Summary of durability advantages

4 Conclusions

This paper has detailed some of the recent research undertaken at the University of Bath. Not only is it demonstrated that fabric formwork can be used to created optimised, low carbon concrete structures, but that its use also facilitates significant improvements in surface durability.

Faced with environmental effects, fabric cast concrete shows a number of advantages. An increase in cement content at the surface, combined with a surface free from voids and blow holes provides a high quality visual finish. A reduction in the volume of large pores at the surface, as suggested by sorptivity data provides a less permeable surface for carbonation and chloride ingress.

In addition, the increased cement content at the surface encourages the formation of Friedel's Salt during chloride attack, further retarding the corrosion process. Increased chloride binding by this higher

cement content prevents depassivation of the steel, which is thus protected. In a similar way, the reduced pore area is considered to contribute to the concrete resistance to carbonation, which helps to prevent the reductions in concrete pH that can lead to corrosion. This web of advantages is illustrated in full in Figure 15.

From the tests outlined in this paper, it is clear that by casting concrete into a permeable mould significant durability benefits can be gained. The 'case hardened' surface zone that is formed may allow designers to beneficially reduce their cover requirements, or, in designs governed by durability concerns, to reduce the specified concrete grade. Such reductions in concrete grade in turn facilitate further savings in embodied energy. For example, if a design required a 50MPa concrete solely to satisfy durability concerns, and if this could be replaced with a 20MPa concrete cast in fabric formwork, the resulting embodied energy savings would be approximately 38%. In conjunction with the material savings already achieved simply by casting optimised shapes and the potential additional carbon savings in using low-carbon cements, it is clear that fabric formwork offers an opportunity for significant embodied energy savings.

In addition, where the concrete surface is required to provide a visual finish, conventional approaches such as increases in cement content may be avoided through the use of fabric formwork. Such an approach further reinforces the specification of fabric cast concrete by its strength requirements only, utilising the construction method to provide the concomitant durability and visual benefits seen in this paper.

The majority of testing undertaken in this paper has made use of one fabric, and further work is currently underway to determine the relative advantages of other available materials in the hope of finding the optimum material that can combine flexibility, a low creep modulus, high strength and a small pore size.

By providing a permeable mould, an advantageous release of water and air during curing results in a cement rich surface zone that provides improved resistance to chloride ingress and carbonation when compared to the same concrete cast into an impermeable mould. These results are supplemented by new investigations into the chemical and structural changes that occur within the surface zone of the concrete. Combined with the processes for design and optimisation of structural elements and the material reductions and carbon savings that will result from this, the durability benefits demonstrated in this paper further cement the thesis that fabric formwork can be used to provide a sustainable future in concrete construction.

5 References

ASTM 2004. C1585. *Standard Test Method for Measurement of Rate of Absorption of Water by Hydraulic-Cement Concretes.* West Conshohocken: ASTM International.

BAMFORTH, P. B. & PRICE, W. F. 1997. An International Review of Chloride Ingress Into Structural Concrete. Scotland: TRL.

BSI 2004. BS EN 1992-1-1. *Eurocode 2: Design of concrete structures - Part 1-1: General rules and rules for buildings.* BSI.

COLLINS, M. P. 1978. Towards a Rational Theory for RC Members in Shear. *Proceedings of ASCE,* 104**,** 649-666.

COLLINS, M. P., MITCHELL, D. & BENTZ, E. C. 2008. Shear Design of Concrete Structures. *The Structural Engineer,* 86**,** 32-39.

DUNSTER, A. M. 2000. Accelerated carbonation testing. London: BRE.

GARBETT, J. 2008. *Bone growth analogy for optimising flexibly fomed concrete beams.* MEng MEng, University of Bath.

GUMMERSON, R. J., HOFF, W. D., HAWKES, R., HOLLAND, G. N. & MOORE, W. S. 1979. Unsaturated water flow within porous materials observed by NMR Imaging. *Nature,* 281**,** 56-57.

HALL, C. 1989. Water sorptivity of mortars and concretes: A Review. *Magazine of Concrete Research,* 41**,** 51-61.

HALL, C. 2007. Anomalous diffusion in unsaturated flow: Fact or Fiction? *Cement and Concrete Research,* 37**,** 378-385.

HAMMOND, G. P. & JONES, C. I. 2008. Embodied energy and carbon in construction materials. *Proceedings of the Institution of Civil Engineers: Energy,* In Press.

LIANG, M. T., QU, W. & C-H, L. 2002. Mathematical modeling and prediction of concrete carbonation and its applications. *Marine and Science Technology,* 10**,** 128-135.

LOCKINGTON, D. & PARLANGE, J. Y. 2003. Anomalous water absorption in porous materials. *Journal of Physics D: Applied Physics,* 36**,** 760-767.

MCCARTHY, M. J., GIANNAKOU, A. & JONES, M. R. 2001. Specifying concrete for chloride environments using controlled permeability formwork. *Materials and Structures,* 34**,** 566-576.

NERVI, P. L. 1956. *Structures*, FW Dodge Corp.

NORDTEST 1989. NT BUILD 357. *Concrete, repairing materials and protective coating: Udc carbonation resistance.*

NORDTEST 1995a. NT BUILD 208. *Concrete, hardened: Chloride content by volhard titration.* Nordtest.

NORDTEST 1995b. NT BUILD 443. *Concrete, hardened: Accelerated chloride penetration.* Nordtest.

ORR, J., DARBY, A., IBELL, T. & EVERNDEN, M. 2011a. Fibre reinforced polymer grids as shear reinforcement in fabric formed concrete beams. *Advanced Composites in Construction 2011.* Warwick, UK.

ORR, J. J., DARBY, A. P., IBELL, T. J. & EVERNDEN, M. 2012a. Durability enhancements using fabric formwork. *fib symposium: Concrete structures for Sustainable Community.* Stockholm.

ORR, J. J., DARBY, A. P., IBELL, T. J. & EVERNDEN, M. 2012b. Fabric formwork for ultra high performance fibre reinforced concrete structures. *fib symposium: Concrete structures for Sustainable Community.* Stockholm.

ORR, J. J., DARBY, A. P., IBELL, T. J., EVERNDEN, M. C. & OTLET, M. 2011b. Concrete structures using fabric formwork. *The Structural Engineer,* 89**,** 20-26.

ORR, J. J., DARBY, A. P., IBELL, T. J., LAVA, P. & DEBRUYNE, D. 2012c. The shear behaviour of non-prismatic concrete beams determined using digital image correlation (submitted for publication). *In:* DIRCKX, J. (ed.) *5th International Conference on Optical Measurement Techniques for Structures and Systems 2012.* Antwerp, Belgium.

SCHIESSL, P. & LAY, S. 2005. Inlfence of concrete composition. *In:* HANS, B. (ed.) *Corrosion in Reinforced Concrete Structures.* Cambridge: Woodhead Publishing.

STEFFENS, A., DINKLER, D. & AHRENS, H. 2002. Modeling carbonation for corrosion risk prediction of concrete structures. *Cement and Concrete Research,* 32**,** 935-941.

TANS, P. 2010. *Trends in Carbon Dioxide* [Online]. US Department of Commerce National Oceanic and Atmospheric Administration, Earth System Research Laboratory. Available: http://www.esrl.noaa.gov/gmd/ccgg/trends [Accessed 11/07/10].

TAYLOR, S. C., HOFF, W. D. & WILSON, M. A. G., K M 1999. Anomalous water transport properties of Portland and blended cement-based materials. *Journal of Material Science Letters,* 18**,** 1925-1927.

USGS 2008. Cement statistics. *In:* KELLY, T. D., MATOS, G.R. (ed.) *Historical statistics for mineral and material commodities in the United States.* USGS.

USGS. 2011. *Minerals Information* [Online]. US DoI, USGS. Available: http://minerals.usgs.gov/minerals/ [Accessed 01/01 2011].

WRI 2005. Carbon Dioxide Emissions by Source 2005. Earthtrends Data Tables: Climate and Atmosphere.

YUAN, Q., SHI, C., SCHUTTER, G., AUDENAERT, K. & DENG, D. 2009. Chloride binding of cement-based materials subjected to external chloride environment - A review. *Construction and Building Materials,* 23**,** 1-13.